



HAL
open science

Development of anti-corrosion coating based on phosphorylated ethyl cellulose microcapsules

Ayoub Ouarga, Hassan Noukrati, Itziar Iraola-Arregui, Allal Barroug, Hicham Ben Youcef, Abdelhamid Elaïssari

► **To cite this version:**

Ayoub Ouarga, Hassan Noukrati, Itziar Iraola-Arregui, Allal Barroug, Hicham Ben Youcef, et al.. Development of anti-corrosion coating based on phosphorylated ethyl cellulose microcapsules. Progress in Organic Coatings, 2020, 148, pp.105885. 10.1016/j.porgcoat.2020.105885 . hal-02986981

HAL Id: hal-02986981

<https://hal.science/hal-02986981>

Submitted on 9 Nov 2023

HAL is a multi-disciplinary open access archive for the deposit and dissemination of scientific research documents, whether they are published or not. The documents may come from teaching and research institutions in France or abroad, or from public or private research centers.

L'archive ouverte pluridisciplinaire **HAL**, est destinée au dépôt et à la diffusion de documents scientifiques de niveau recherche, publiés ou non, émanant des établissements d'enseignement et de recherche français ou étrangers, des laboratoires publics ou privés.

Development of Anti-Corrosion Coating Based on Phosphorylated Ethyl Cellulose Microcapsules

Ayoub Ouarga^{a,b,c}, Hassan Noukrati^a, Itziar Iraola-Arregui^a, Abdelhamid Elaissari^c, Allal Barroug^{a,b}, Hicham Ben youcef^{a,*}

^aMohammed VI Polytechnic University (UM6P), Lot 660 – Hay Moulay Rachid, 43150, Benguerir, Morocco.

^bCadi Ayyad University, FSSM, BP. 2390, 40000 Marrakech, Morocco.

^cUniv Lyon, University Claude Bernard Lyon-1, CNRS, LAGEP-UMR 5007, F-69622 Lyon, France.

*Corresponding author: Email: hicham.benyoucef@um6p.ma, +212 6 516 32 456 (H. Ben youcef)

Abstract

This study reports for the first time the preparation of almond oil-based microcapsules using phosphorylated ethyl cellulose as shell material. Microcapsules of ethyl cellulose (EC) and phosphorylated ethyl cellulose (P-EC) containing almond oil as anti-corrosion inhibitor, for end use in self-healing coatings, were prepared by a solvent evaporation method. The results showed that phosphorus content in the modified ethyl cellulose was 6.26 wt.%, the specific surface area reached a high value of $21.4 \text{ m}^2\text{g}^{-1}$ and a char residue of 18 wt.% at 400 °C after thermal degradation. Both prepared EC and P-EC based microcapsules were spherical shape-like. The scanning electron microscope (SEM) images showed that the freeze-drying influences the microcapsules surface morphology. The mean diameter of EC and P-EC microcapsules was about 140 μm and 150 μm , respectively. Anti-corrosion properties of prepared epoxy-based coatings loaded with microcapsules on the mild steel substrate were evaluated for 28 days using a simple salt spray test. The sample containing P-EC microcapsules showed the best anticorrosion resistance. The functionalization of the ethyl cellulose microcapsules shell with phosphonate groups can improve further the anti-corrosion resistance, the flame-retardant ability and the metal chelating properties of the final coatings.

Keywords: Anti-corrosion coating; biopolymers; ethyl cellulose; microencapsulation; phosphorylation; self-healing

Highlights

- Novel phosphorylated ethyl cellulose based microcapsules containing almond oil were prepared.
- Phosphorylation induced an increase of the carbonaceous residue formation and an improvement of heat resistance
- Addition of phosphorylated ethyl cellulose based microcapsules to coatings enhances their anti-corrosion performance.

1. Introduction

Corrosion is a widespread thermodynamically governed natural phenomenon that can deteriorate materials generally, and metals specifically. It is a chemical process that breaks down materials gradually by electron exchange and new molecules formation [1]. At present, enormous investment is allocated all over the world to protect materials from corrosion, especially metals. In 2016, the global cost of damage caused by corrosion was estimated to be US \$2.5 trillion [2]. To prevent and protect metals against corrosion, many methods exist and are used commonly. For instance, the cathodic protection and the anti-corrosion coating methods. However, these methods are costly and need periodic replacement of the sacrificial anode or renewal of the coating, implying the use of chemicals with high toxicity and harmful effect on the environment [3-6]. So far, new approaches have been adopted to protect materials from corrosion, especially self-healing techniques, which allow cost-effective corrosion protection in more environmentally friendly approaches [7].

The self-healing phenomenon can be classified into two types: intrinsic and extrinsic, depending on the way of healing. The first type is based on special characteristics of the polymer that allow repairing under certain stimuli. In the second type, extrinsic self-healing, the polymeric matrix is not healable. Thus, the healing agent must be encapsulated and pre-embedded in the bulk material [8, 9]. The microencapsulation of natural self-healing agents is an active research area. A significant part of these investigations is dedicated to specific materials that protect and cover the defects of metal coatings caused by several surrounding conditions and stimuli [10-16]. Microencapsulation technology has been considered a relevant method to develop new and versatile smart materials for different applications, especially in the field of self-healing composite materials. Within the coating application, microencapsulation allows the protection of solid, liquid or gas materials using polymeric

shells. This technology is considered as the first and primordial step in the preparation process of extrinsic self-healing materials [16-19].

Microcapsules for anti-corrosion coating applications are based on core materials containing an anti-corrosion healing agent. Then, microcapsules must be embedded in paints as part of the anti-corrosion coating [12, 20]. Among shell materials for microencapsulation, cellulose and derivatives were widely used for diverse applications. In fact, cellulose and derivative materials are sustainable, biocompatible, non-toxic and possess good chemical and mechanical properties, that promote their use in the microcapsules preparation [21-23]. The main approaches for the preparation of these materials for microencapsulation include emulsion-based methods such as temperature-induced phase separation, emulsion solvent evaporation and solvent evaporation from oil-in-water emulsion [24, 25].

Vegetable oils have received recurrent attention in the last decades due to their eco-friendliness, low cost and availability which make them suitable materials for several purposes, including: food industry, paints and anticorrosion applications [26, 27]. Linseed, soybean and tung, are the most studied vegetable oils due to their abundance and ease of extraction from renewable and sustainable resources [28]. They are used in edible applications such as food industry, as well as non-edible applications such as self-healing materials [10, 14, 28, 29]. In this context, we report hereby almond oil as a promising green corrosion inhibitor. The chemical structure of vegetable oils is generally composed of 90 to 98 % of triglycerides, which are esters containing multiple fatty acids, that comprise oleic, linoleic, alpha linoleic, palmitic, palmitoleic and stearic acids [30]. Almond oil is generally a combination of 68 % oleic acid, 25 % linolenic acid and 4 % palmitic acid. High content of double bonds-rich fatty acid as oleic acid offers this material the ability to protect metals against corrosion by free radical auto-oxidation reaction mechanism of the double bonds with oxygen [31-34].

Our research work aimed to incorporate almond oil in the core of microcapsules based on ethyl cellulose and phosphorylated ethyl cellulose as shell materials, and their subsequent use in a self-healing anti-corrosion coating. For this purpose, ethyl cellulose bearing phosphonate groups was prepared by phosphorylation reaction under specific conditions. We report for the first time, microcapsules combining phosphorylated ethyl cellulose with almond oil in self-healing coating. Almond oil was selected due to its composition and corrosion inhibition abilities. The resulting modified ethyl cellulose and microcapsules were subjected to several characterization techniques. The effect of the phosphonate group in

combination with the almond oil was investigated as anti-corrosion additives. Thus, metallic samples having a coating loaded with microcapsules were subjected to a mechanical scratch and their corrosion resistance was monitored via salt spray tests.

2. Experimental

2.1 Materials

The reagents used for the materials preparation were ethyl cellulose powder (viscosity 10 cP, measured as a 5 % vol in toluene/ethanol 80:20 (vol), extent of labeling: 48 % ethoxyl), urea powder and sodium dodecyl sulfate (SDS) (Sigma Aldrich), ethyl acetate (EA) (Somaprol), orthophosphoric acid (85 %), methanol (Merck KGaA) and Sodium hydroxide (VWR). Sweet almond oil was purchased from a drugstore and used as a core material for microcapsules. All chemicals were analytical reagents grade and were used as received.

2.2 Ethyl Cellulose phosphorylation

The ethyl cellulose phosphorylation was performed under homogeneous conditions using phosphoric acid in molten urea [35, 36]. 5 g of ethyl cellulose were dispersed under stirring in 25.7 g of phosphoric acid H_3PO_4 and 7 g of distilled water. 16 g of urea were melted in a two-necked flask attached to a condenser at 140 °C. The dispersion was added to the molten urea while the temperature was adjusted to 150 °C, and the reaction was carried out for 30 minutes. The obtained combination was then dissolved in a solution of NaOH, precipitated in methanol, filtered, washed and purified via membrane-based dialysis process in distilled water. Finally, the phosphorylated ethyl cellulose was freeze dried for 72 hours.

2.3 Preparation of microcapsules

In order to prepare almond oil-filled microcapsules using ethyl cellulose (EC) or phosphorylated ethyl cellulose (P-EC) as shell material, we followed the procedure described elsewhere [25]. The selected microencapsulation method is considered as a two-stage solvent evaporation method. The first preparation, oil phase, consists on dissolving the ethyl cellulose powder or the phosphorylated ethyl cellulose in ethyl acetate (90 wt.%) under magnetic stirring of 650 rpm at ambient temperature. The dissolution was done in 2 hours. Almond oil was then added gradually to the above-mentioned solution. The system was kept under magnetic stirring at room temperature for further 30 minutes. For the second preparation, water phase, an aqueous solution of 1 wt.% sodium dodecyl sulfate (SDS) was prepared. The oil phase was then added drop wise to the water phase under mechanical

mixing at 60 °C for 90 minutes. The mixture was freeze-dried then washed with distilled water and filtered to remove the remaining surfactant and generate the final microcapsules. Obtained microcapsules based on EC and P-EC are designated by MC and P-MC, respectively.

2.4 Characterization

The surface morphology of ethyl cellulose (EC) and phosphorylated cellulose (P-EC) were observed by scanning electron microscopy (SEM) using a Quanta FEG 250. The presence of phosphorus (P) in the P-EC was examined by Energy Dispersive X-ray spectroscopy (EDX) using IDFix software by SAMx attached to the Quanta FEG 250 electron microscope.

Fourier Transform Infrared (FTIR) Spectra of initial raw materials, phosphorylated ethyl cellulose and prepared microcapsules were recorded by a PerkinElmer FTIR spectrophotometer (Wellesley, MA, United States), collecting 16 scans in the 4000-600 cm⁻¹ range with 4 cm⁻¹ resolution.

The phosphorus (P) content of the modified ethyl cellulose was measured using the inductively coupled plasma optical emission spectrometry method (ICP-OES), on Agilent 5110 ICP-OES Instrument. The specific surface area of the EC and P-EC powders was determined by the BET method, using nitrogen adsorption measurements (Micromeritics Gemini VII 1014 Instrument).

The prepared microcapsules were observed by an optical microscope (Nikon metallographic microscope LV100ND) under 20-100 X magnification. The microcapsules morphology and shell thickness were examined using a scanning electron microscope (Philips XL 40 ESEM). The microcapsules size was determined by a laser particle size analyzer (Malvern, Mastersizer 2000).

Microcapsules thermal stability was evaluated by means of thermogravimetric analysis (TGA) technique using a thermogravimetric analyzer (Model –TGA 5500, Discovery series, TA Instruments, United States). The tests were performed under a nitrogen atmosphere and heating from room temperature up to 700 °C using a heating rate of 10 °C/min.

The oil content in the microcapsules was determined by solvent extraction. Weighed mass of microcapsules (m₁) was mixed with 200 mL of n-hexane and the mixture was sonicated for 10 min. The suspension was then filtrated, and the solid filtrate was then collected and dried in an oven at 50 °C until a constant weight is measured (m₂). The oil content encapsulated in the microcapsules can be determined using the following equation:

$$\text{oil content (\%)} = \frac{(m_1 - m_2)}{m_1} 100 \%$$

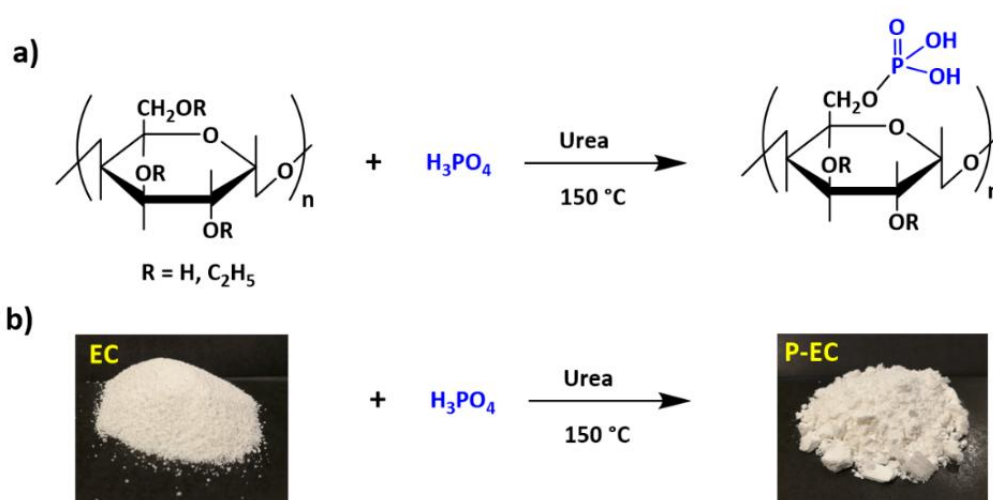
2.5 Preparation of coating samples containing microcapsules

Mild steel substrates with a dimension of 100 × 45 × 1 mm were ground to 1000-grits with abrasive paper, degreased in acetone and dried in air. 15 wt.% of microcapsules were gently dispersed into the epoxy resin under manual mixing using spatula. A stoichiometric amount of the hardener was then added to the mixture. The coatings were applied on degreased and polished steel substrates using a manual film applicator. The coated steel panels were dried overnight in a fume hood at room temperature. The average thickness of dry film samples was measured as 500 ± 15 μm.

3. Results and Discussion

3.1 Phosphorylated Ethyl-Cellulose characteristics

Phosphorylated polysaccharides are a very interesting class of materials that can exhibit practical properties (e.g., biocompatibility, bactericidal activity, bio absorbability, and metal-chelating). In this study, P-EC was prepared by the phosphorylation of the EC using the procedure depicted in the scheme 1. The phosphorylation protocol was performed at 150 °C to activate the attachment of phosphonate groups in order to obtain a high degree of substitution [37]. Urea was used in excess to fulfil a dual role in the functionalization procedure. On one hand it promotes the phosphorylation reaction, and on the other hand it protects the polymeric matrix at high temperature from degradation in the aggressive acidic conditions (10.7 M) [38].



Scheme 1. a) Schematic of the phosphorylation reaction of the ethyl cellulose (EC). **b)** Visual aspect of ethyl cellulose (EC) and phosphorylated ethyl cellulose (P-EC).

These conditions and the drying technique did not affect the visual powder like aspect of the obtained P-EC final product (scheme 1). Interestingly, the specific surface area of P-EC adsorbent, determined by the N₂-BET method, was highly increased compared with that of the native ethyl cellulose. In fact, the obtained results were 1.1 m²g⁻¹ for EC and 21.4 m²g⁻¹ for P-EC.

It was expected that the phosphorylation reaction will induce a change in the intermolecular interactions between the P-EC chains, thus, modifying the compactness properties due to steric effect and surface charge modification. The polysaccharide samples were sputter coated with copper (Cu) before SEM-EDX analysis. The SEM images of the lyophilized P-EC powder showed a spongy aspect after freeze drying, as can be depicted in (Fig. 1 (a-b)). This new roughness may be the reason for the measured specific surface area increase. The phosphorus element (P) mapping image showed almost uniform distribution in the characterized sample (Fig.1(d)). Even if the mapped sample is rough, the obtained result supports the effective chemical modification and the phosphorylation of the ethyl cellulose.

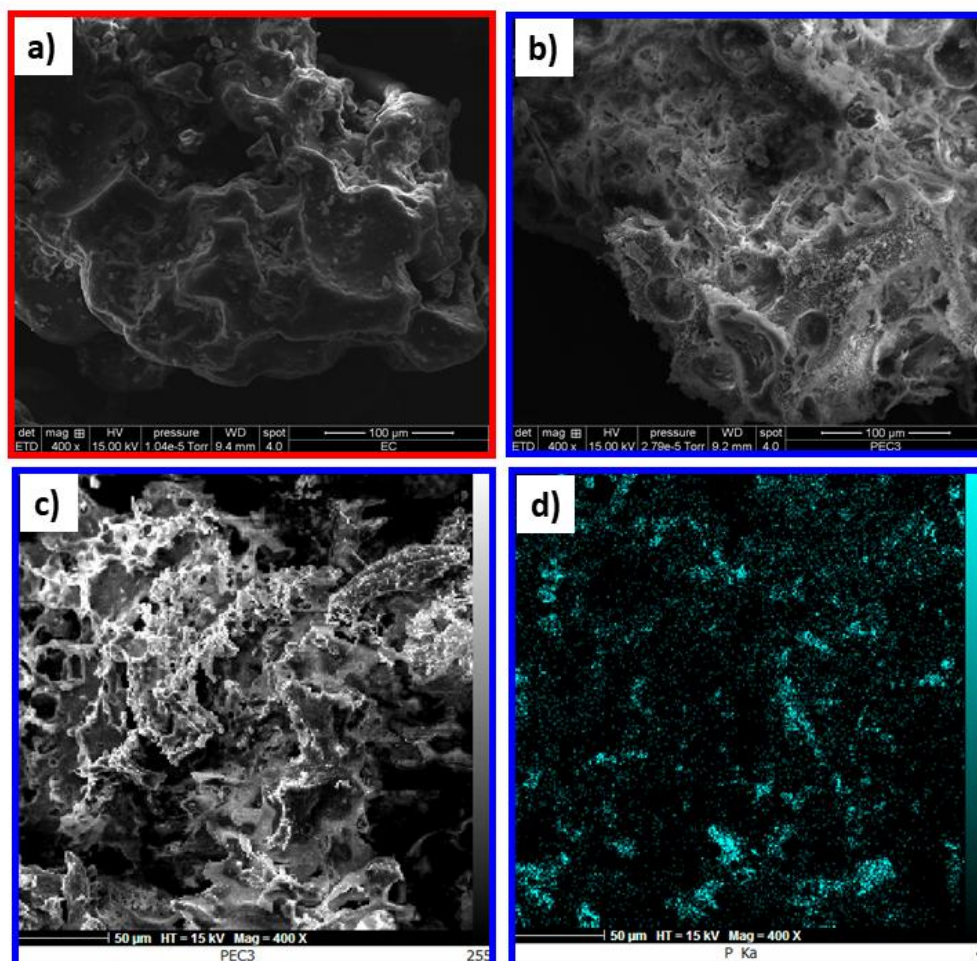


Fig. 1. SEM micrographs of (a) ethyl cellulose (EC) and (b-c) phosphorylated cellulose (P-EC).

(d) Mapping of phosphorus element for phosphorylated ethyl cellulose (c).

The ethyl cellulose phosphorylation was confirmed by FTIR measurements (Fig. 2). The FTIR spectrum of the modified ethyl cellulose showed the characteristic peaks of both native ethyl cellulose and new peaks related to phosphorus groups. The peak at 800 cm^{-1} is assigned to P-O-C groups, and another broad peak at 1630 cm^{-1} is related to O=P-OH deformation vibrations. Moreover, the phosphorus content was confirmed by inductively coupled plasma - optical emission spectrometry (ICP-OES) analysis and the modified EC contains 6.26 wt.% P.

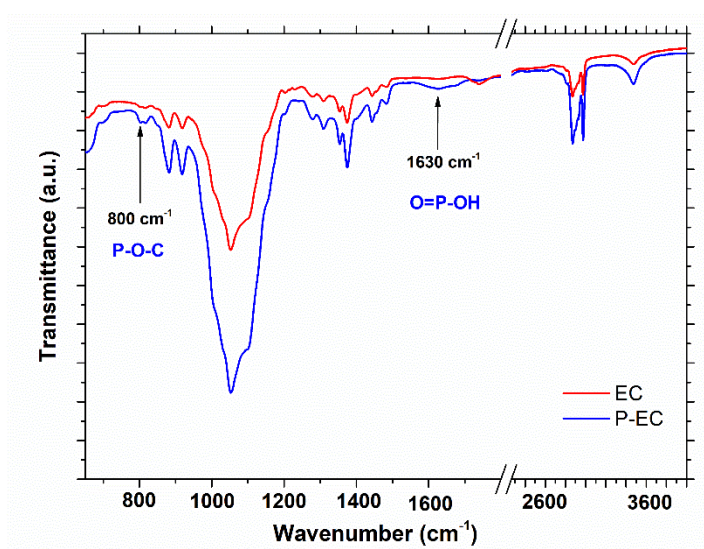


Fig. 2. FTIR spectra of ethyl cellulose (EC) and phosphorylated ethyl cellulose (P-EC).

Figure 3 shows the main characteristics of thermal degradation of native and phosphorylated ethyl cellulose, determined by thermogravimetric analysis.

As seen from (Fig. 3), native ethyl cellulose shows a maximum weight loss rate at $362\text{ }^{\circ}\text{C}$, whereas this appeared at $304\text{ }^{\circ}\text{C}$ for the phosphorylated ethyl cellulose. Thus, the introduced structures containing phosphorus catalyze the polymer's thermal degradation and carbonization, so that the main degradation process starts for phosphorylated ethyl cellulose at a temperature of $213\text{ }^{\circ}\text{C}$ compared to the corresponding native ethyl cellulose which starts at $273\text{ }^{\circ}\text{C}$ (Table 1). The phosphorylated ethyl cellulose loses 20 wt.% at $281\text{ }^{\circ}\text{C}$, whereas for the native ethyl cellulose, the same weight loss is observed at a higher temperature of $338\text{ }^{\circ}\text{C}$.

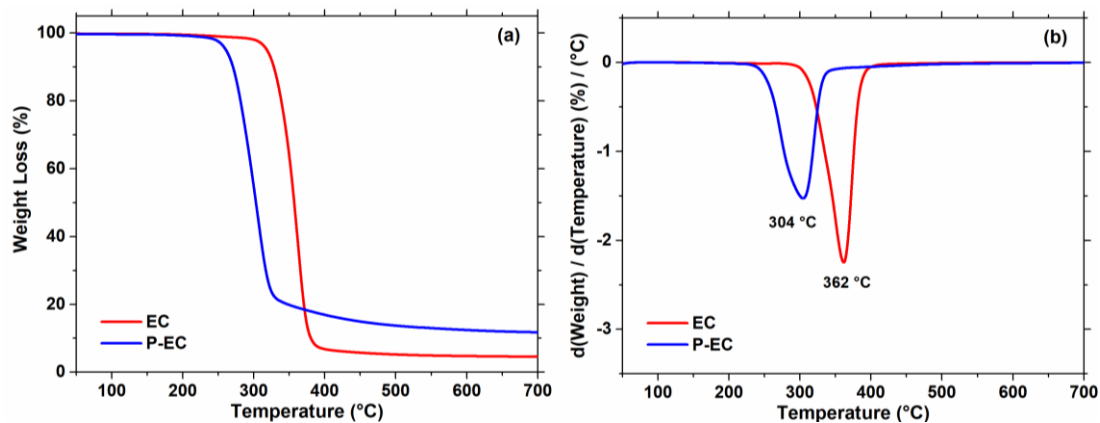


Fig. 3: Thermal degradation of native EC and P-EC. (a) TGA weight loss curves, and (b) weight loss first derivative curves.

It was noticed that, the weight loss of the P-EC is considerably lower compared to the native EC, and a difference of 17 wt.% was observed at 400 °C. The residue reaches 11.7 wt.% for the P-EC and 4.3 wt.% for native EC at 700 °C, which mean a difference of 7.4 wt.% (Table 1). The native EC undergoes complete decomposition at 406 °C whereas the phosphorylated one underwent it at 350 °C. The observed thermal behavior of the P-EC is a clear indicator of a flame retardancy polymer material, where the phosphonate groups act as a promoter for more char residue at high temperature [38, 39]. Only 6.26 % weight amount of phosphorus in the P-EC induced a clear modification of its pyrolysis process reducing the flammable volatiles amount and increasing the carbonaceous residue formation which indicates its higher heat resistance.

Table 1. Specific surface area and thermal degradation characteristic properties of ethyl cellulose (EC) and phosphorylated cellulose (P-EC).

	Specific surface area*	Degradation temperature onset**	Degradation temperature**	Final weight residue**
	m^2g^{-1}	$^{\circ}\text{C}$	$^{\circ}\text{C}$	%
EC	1.1	213	304	4.3
P-EC	21.4	273	362	11.7

* Determined by BET

** Measured by TGA

3.2 Microcapsules morphology and size distribution

Microcapsules based on ethyl cellulose (MC) and phosphorylated ethyl cellulose (P-MC) were prepared successfully. The content of the almond oil in the microcapsules was determined by extraction in n-hexane. The average oil content in the microcapsules was evaluated to be 58% and 61% for the MC and P-MC, respectively. Optical microscope images and SEM micrographs show that the obtained microcapsules have a spherical shape without any physical and strong inter-capsule bonding (Fig. 4).

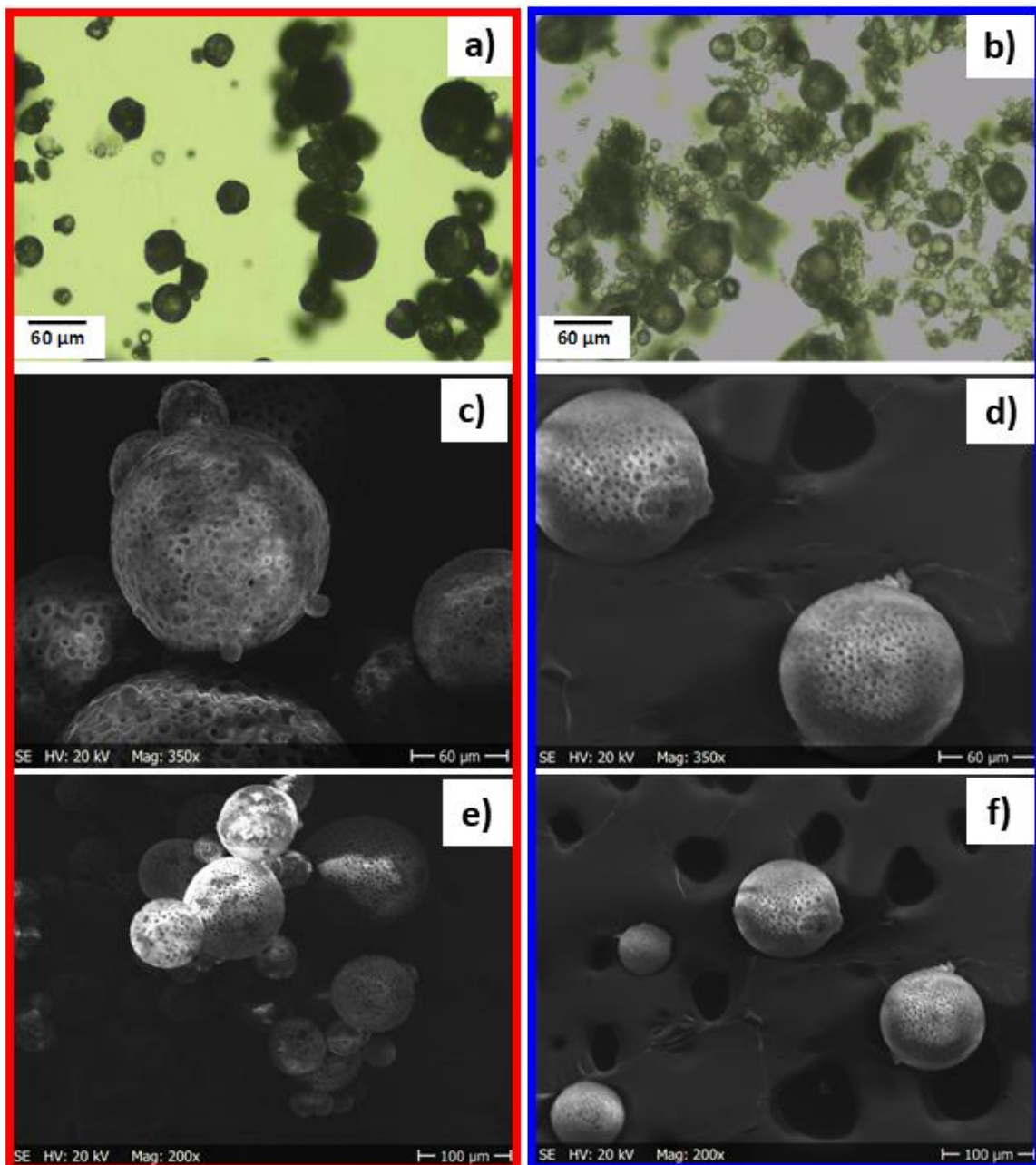


Fig. 4. Optical microscope images of almond oil-filled microcapsules using **(a)** EC and **(b)** P-

EC as shell material. SEM micrographs of almond oil-filled microcapsules using **(c, e)** EC and **(d, f)** P-EC as shell material.

Moreover, microcapsules seem to have a rough shell surface with some residues on their top most likely due to agglomerations of the EC or P-EC which did not participate to the shell formation. Optical micrographs show the evidence of high dispersity of the size of the prepared microcapsules. In fact, the average diameter of almond oil microcapsules based native EC and phosphorylated EC is about 140 μm and 150 μm , respectively (Fig. 5).

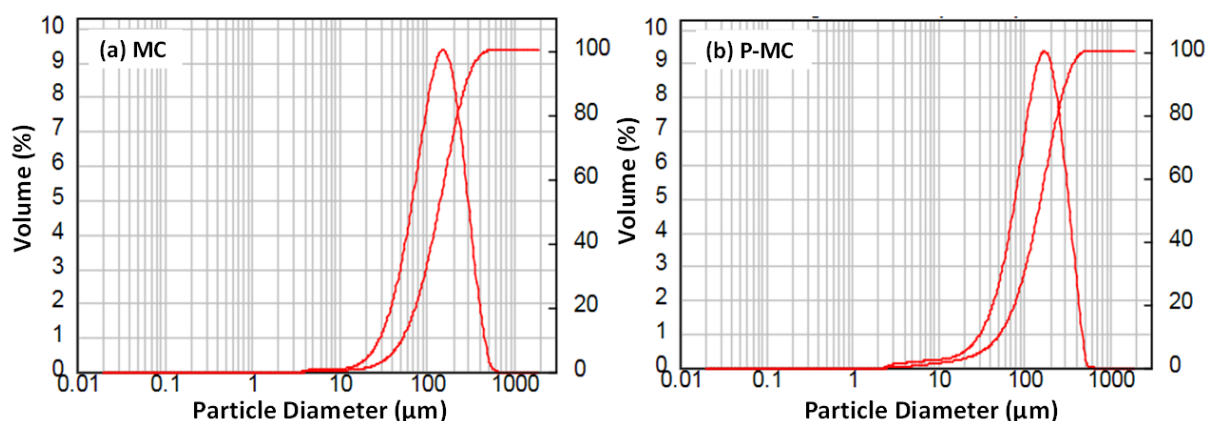


Fig. 5. (a) Size distribution of ethyl cellulose-based microcapsules (MC) containing Almond oil, and **(b)** Size distribution of phosphorylated ethyl cellulose-based microcapsules (P-MC) containing Almond oil.

The absence of almond oil around the microcapsules on the optical micrographs confirms the good oil encapsulation inside the shell material in both ethyl cellulose and phosphorylated ethyl cellulose. SEM micrographs did not show significant dissimilarity of surface morphology for microcapsules prepared using different shell materials, which makes clear the non-dependence of microcapsules features on shell material nature. Still, both non-phosphorylated and phosphorylated microcapsules have crater features on their surfaces and a golf ball-like morphology. The microcapsule morphology and final shape are depending on several parameters, e.g., core-shell materials, temperature, mixing mode, emulsifier and drying method. The lyophilization (freeze-drying) procedure is suspected to be the main factor responsible for the crater features observed on the surface of the obtained microcapsules. In fact, this drying method was previously pointed out to be the main cause of the porous structure on the surface of the obtained microcapsules [40]. This shape might affect self-healing efficiency and microcapsule's long-term stability. Hence, the craters will increase the exposition of the active ingredient encapsulated to the atmosphere,

thus lowering the protection of the core material. Interestingly, the remaining microcapsules (i.e., MC and P-MC) were stable over several months inside a desiccator without any noticeable changes. The same microcapsules were prone to agglomeration when left for a prolonged shelf exposure under ambient air humidity conditions. In fact, the hydrophilicity of the shell materials is promoting the increase of water content, hence the observed tendency to agglomeration.

3.3 Core-Shell Microcapsules FTIR Analysis

For chemical characterization of the core, shell and microcapsules, attenuated total reflectance-Fourier transform infrared (ATR-FTIR) spectroscopy was used (Fig. 6).

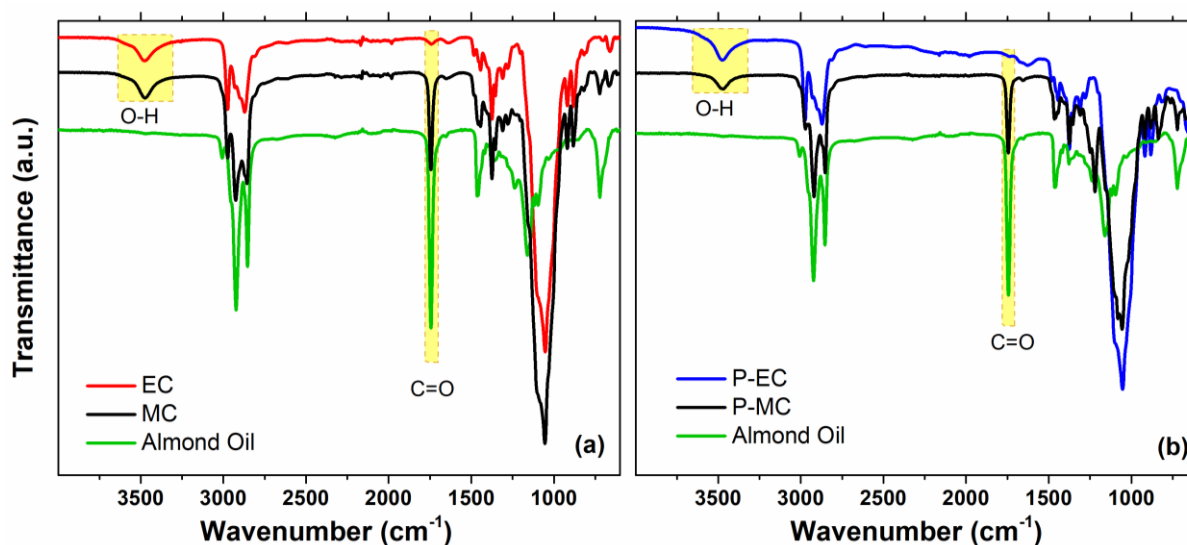


Fig. 6. (a) FTIR spectra of ethyl cellulose microcapsules (MC), almond oil and ethyl cellulose (EC). **(b)** FTIR spectra of phosphorylated ethyl cellulose microcapsules (P-MC), almond oil and phosphorylated ethyl cellulose (P-EC).

The infrared spectra of almond oil showed sharp peaks at 2921 cm⁻¹, 2849 cm⁻¹, 1462 cm⁻¹ and 723 cm⁻¹ related to the methylene groups. Peaks corresponding to the methyl group vibration were observed at 1464 cm⁻¹ and 1375 cm⁻¹. The characteristic peak of olefinic double bonds is seen at 3009 cm⁻¹. The triglyceride ester groups appeared at 1743 cm⁻¹, 1235 cm⁻¹, 1159 cm⁻¹ and 1095 cm⁻¹ [41-43]. The phosphorylated microcapsules FTIR spectra reveal the appearance of new small peaks at 810 cm⁻¹ and 1630 cm⁻¹ corresponding respectively to P-O-C and O=P-OH group, due to the presence of the phosphorus in the P-EC shell.

The microcapsules infrared spectra contain all the characteristic peaks of the core material (Almond oil) and shell material (in yellow in fig.7). This gives a clear confirmation that the

microencapsulation was correctly carried out using both ethyl cellulose and phosphorylated ethyl cellulose as shell materials. Moreover, no bands related to SDS were observed either for the MC and P-MC based microcapsules, hence, the efficiency of the cleaning procedure during the preparation step is proved.

3.4 Thermal Analysis

The thermal stability of the prepared microcapsules was investigated by thermogravimetric analysis (TGA) and the obtained results are presented in Fig. 7. The prepared microcapsules (phosphorylated and non-phosphorylated) exhibit two stages of weight loss. The almond oil microcapsules show two stages at 206–290 °C and 290–450 °C, which correspond to the decompositions of ethyl cellulose shell and the almond oil core, respectively. The thermal degradation shows an overlapping temperature range of the core and shell materials which limits the accurate determination of the percentage of each component.

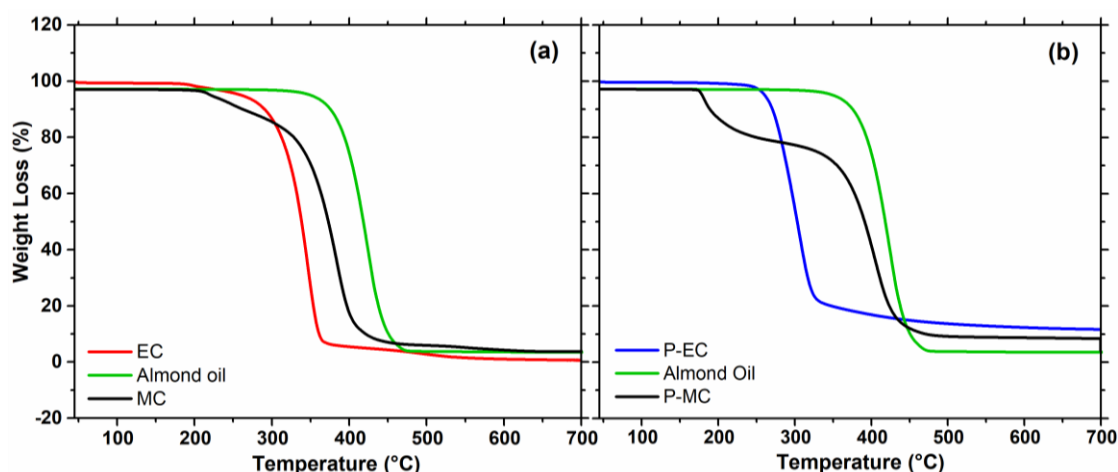


Fig. 7. (a) TGA weight loss curves of native ethyl cellulose (EC), almond oil and full microcapsules (MC). **(b)** TGA weight loss curves of phosphorylated ethyl cellulose (P-EC), almond oil and full phosphorylated microcapsules (P-MC).

The phosphorylated microcapsules thermogram shows an initial stage weight loss at 180-290 °C related to the decomposition of phosphorylated ethyl cellulose. The second stage weight loss supporting the decomposition of almond oil was observed between 290 °C and 500 °C. It is worth to note that the thermal degradation of the MC and P-MC microcapsules resulted in a final residue of 0.5 % and 5.2%, respectively. The TGA study confirmed the absence of the SDS material within the MC and P-MC microcapsules, which is typically characterized by an onset degradation temperature around 162 °C and a maximum degradation temperature around 218°C. It is worth commenting that the flame retardancy character of the used P-EC

is still clearly observed for the resulting prepared microcapsules. Even at a small percentage, the phosphorus in the microcapsule shell induced and increase of the carbonaceous residue formation.

3.5 Salt spray test results

To evaluate the self-healing abilities and corrosion resistance of the prepared microcapsules, a salt spray test was performed on metallic substrates. The visual aspect progression during the study of the scratched areas on coated blank, MC and P-MC based samples is shown in (Fig. 8). To begin with, both scratched microcapsules loaded coatings showed a marked effectiveness in preventing corrosion compared to blank epoxy coating during the first week of test. However, all samples showed corroded zones at different stages across the scratched region after 28 days of the spray test using the 3.5 wt.% NaCl solution. In fact, the corroded zone was more evident on the pure epoxy resin coated sample compared to samples coated with epoxy resin loaded with microcapsules. In the case of blank samples, the rust was already propagated upon most of the scratch area after only 7 days of salt spray exposure and continued to develop until the end of the test. Moreover, it was clearly visible that the corrosion was spreading even more in between the coating and the metal surface at the end of the test. While in the case of samples containing non-phosphorylated microcapsules (MC), the corrosion emerged on the scratch center starting from day 7 and continued to progress showing a better anti-corrosion resistance compared to the blank samples. The study showed also that, the corrosion process did not visibly occur in the sample containing phosphorylated microcapsules (P-MC) until day 28, which reveals a better anti-corrosion resistance in comparison to both blank and MC containing samples. Considering the component of the P-MC compared with the MC, the phosphonate group is playing a crucial role in the observed anticorrosion performances. It is well known that phosphorus-containing compounds promote the anti-corrosion effects owing mostly to their excellent adhesion ability [44]. In addition to the strong interfacial interactions of phosphonate groups with the metal substrate, additional interactions are expected with the functional groups of the fatty acids of the core materials. Thus, there is a synergic effect between the phosphonate groups and the fatty acids of the almond oil integrated within the prepared coatings. In optimal conditions, a strong interaction between the P-O^- functional groups and the metal ions M^{n+} from the metal substrate is occurring [44]. Furthermore, the hydroxyl and

phosphonate groups on the P-EC can interact via hydrogen bonding with the triglycerides constituted of fatty acids.

Samples coding	Salt spray exposure time (day)			
	1 day	7 days	14 days	28 days
a) Blank				
b) MC				
c) P-MC				

Fig. 8. Optical photographs of scratched coated mild steel samples (a,b,c) after various exposure times (1, 7, 14 and 28 days) to salt spray with 3.5 wt.% NaCl solution. a) blank, without microcapsules b) coating with ethyl cellulose based microcapsule (MC) c) coating with phosphorylated ethyl cellulose microcapsules (P-MC).

4. Conclusions

Phosphorylated ethyl cellulose was successfully obtained through a phosphorylation reaction using phosphoric acid in the presence of molten urea. ICP-OES analysis confirm a content of 6.26 wt.% of phosphorus in the structure of P-EC. The functionalization of the EC promoted its flame retardancy behavior as revealed by the TGA analysis. Moreover, the specific surface area of P-EC showed an increase by a factor of 20 compare to that of native EC. The almond oil encapsulation was carried out successfully and the microcapsules showed a practical thermal stability window for the targeted application. The self-healing and anti-corrosion properties of prepared microcapsules were evaluated by a salt spray test on

scratched epoxy-based coatings. The results revealed that the coating containing phosphorylated microcapsules had a higher corrosion resistance compared to both blank coating and the coating loaded with non-phosphorylated microcapsules over a 4 weeks test. The phosphorylated microcapsules formulated in this work are presented as a proof of concept. To the best of our knowledge, this is the first attempt to prepare almond oil microcapsules using ethyl cellulose and phosphorylated ethyl cellulose as shell materials. These microcontainers approach seems to be promising and could potentially be used in different green and sustainable applications to enhance materials properties such as durability, biodegradability, metal chelating and flame retardancy. Further investigations and tests on the influence of the degree of phosphorylation on the performances of these materials are currently in progress and should be the subject of a forthcoming publication.

CRedit author statement

Ayoub Ouarga: conceptualisation, Writing-original draft preparation. **Hassan Noukrati:** investigation, Supervision. **Itziar Iraola-Arreguia:** Formal analysis, review. **Abdelhamid Elaissari:** Supervision, review & editing. **Allal Barroug:** Supervision, review & editing. **Hicham Ben Youcef:** Writing - original draft - review & editing.

References

- [1] E. Katoueizadeh, S.M. Zebarjad, K. Janghorban, Investigating the effect of synthesis conditions on the formation of urea–formaldehyde microcapsules, *Journal of Materials Research and Technology*, 8 (2019) 541-552.
- [2] G. Koch, 1 - Cost of corrosion, in: A.M. El-Sherik (Ed.) *Trends in Oil and Gas Corrosion Research and Technologies*, Woodhead Publishing, Boston, 2017, pp. 3-30.
- [3] L.T. Popoola, A.S. Grema, G.K. Latinwo, B. Gutti, A.S. Balogun, Corrosion problems during oil and gas production and its mitigation, *International Journal of Industrial Chemistry*, 4 (2013) 35.
- [4] D.G. Shchukin, M. Zheludkevich, K. Yasakau, S. Lamaka, M.G.S. Ferreira, H. Möhwald, Layer-by-Layer Assembled Nanocontainers for Self-Healing Corrosion Protection, *Advanced Materials*, 18 (2006) 1672-1678.
- [5] E.W. Brooman, Modifying organic coatings to provide corrosion resistance—Part I: Background and general principles, *Metal Finishing*, 100 (2002) 48-53.
- [6] I.J. Zvonkina, M. Hilt, 5 - Strategies for developing multi-functional, self-healing coatings for corrosion prevention and other functions, in: A.S.H. Makhlof (Ed.) *Handbook of*

- Smart Coatings for Materials Protection, Woodhead Publishing, 2014, pp. 105-120.
- [7] V. Mittal, Self-healing anti-corrosion coatings for applications in structural and petrochemical engineering, in, 2014, pp. 183-197.
- [8] S. An, M.W. Lee, A.L. Yarin, S.S. Yoon, A review on corrosion-protective extrinsic self-healing: Comparison of microcapsule-based systems and those based on core-shell vascular networks, *Chemical Engineering Journal*, 344 (2018) 206-220.
- [9] R.S. Trask, H.R. Williams, I.P. Bond, Self-healing polymer composites: mimicking nature to enhance performance, *Bioinspiration & Biomimetics*, 2 (2007) 1-9.
- [10] S. Ataei, S.N. Khorasani, R.E. Neisiany, Biofriendly vegetable oil healing agents used for developing self-healing coatings: A review, *Progress in Organic Coatings*, 129 (2019) 77-95.
- [11] M.F. Montemor, Functional and smart coatings for corrosion protection: A review of recent advances, *Surface and Coatings Technology*, 258 (2014) 17-37.
- [12] E. Koh, S. Park, Self-anticorrosion performance efficiency of renewable dimer-acid-based polyol microcapsules containing corrosion inhibitors with two triazole groups, *Progress in Organic Coatings*, 109 (2017) 61-69.
- [13] T. Matsuda, K.B. Kashi, K. Fushimi, V.J. Gelling, Corrosion protection of epoxy coating with pH sensitive microcapsules encapsulating cerium nitrate, *Corrosion Science*, 148 (2019) 188-197.
- [14] H. Li, Y. Cui, Z. Li, Y. Zhu, H. Wang, Fabrication of microcapsules containing dual-functional tung oil and properties suitable for self-healing and self-lubricating coatings, *Progress in Organic Coatings*, 115 (2018) 164-171.
- [15] M.F. Montemor, C. Vicente, Functional self-healing coatings: A new trend in corrosion protection by organic coatings, in: *Encyclopedia of Interfacial Chemistry: Surface Science and Electrochemistry*, Elsevier, 2018, pp. 236-249.
- [16] M. Samadzadeh, S.H. Boura, M. Peikari, S.M. Kasiriha, A. Ashrafi, A review on self-healing coatings based on micro/nanocapsules, *Progress in Organic Coatings*, 68 (2010) 159-164.
- [17] E. Onder, N. Sarier, 2 - Thermal regulation finishes for textiles, in: R. Paul (Ed.) *Functional Finishes for Textiles*, Woodhead Publishing, 2015, pp. 17-98.
- [18] E.N. Brown, S.R. White, N.R. Sottos, Retardation and repair of fatigue cracks in a microcapsule toughened epoxy composite—Part II: In situ self-healing, *Composites Science and Technology*, 65 (2005) 2474-2480.
- [19] C. Suryanarayana, K.C. Rao, D. Kumar, Preparation and characterization of microcapsules containing linseed oil and its use in self-healing coatings, *Progress in*

- Organic Coatings, 63 (2008) 72-78.
- [20] K.A. Bogdanowicz, B. Tylkowski, M. Giamberini, Preparation and Characterization of Light-Sensitive Microcapsules Based on a Liquid Crystalline Polyester, *Langmuir*, 29 (2013) 1601-1608.
- [21] C. Carrick, M. Ruda, B. Pettersson, P.T. Larsson, L. Wågberg, Hollow cellulose capsules from CO₂ saturated cellulose solutions—their preparation and characterization, *RSC Advances*, 3 (2013) 2462-2469.
- [22] S. Prasertmanakit, N. Praphairaksit, W. Chiangthong, N. Muangsin, Ethyl Cellulose Microcapsules for Protecting and Controlled Release of Folic Acid, *AAPS PharmSciTech*, 10 (2009) 1104.
- [23] S.M. Mirabedini, I. Dutil, L. Gauquelin, N. Yan, R.R. Farnood, Preparation of self-healing acrylic latex coatings using novel oil-filled ethyl cellulose microcapsules, *Progress in Organic Coatings*, 85 (2015) 168-177.
- [24] T.L. Rogers, D. Wallick, Reviewing the use of ethylcellulose, methylcellulose and hypromellose in microencapsulation. Part 2: Techniques used to make microcapsules, *Drug Development and Industrial Pharmacy*, 37 (2011) 1259-1271.
- [25] S.M. Mirabedini, I. Dutil, R.R. Farnood, Preparation and characterization of ethyl cellulose-based core-shell microcapsules containing plant oils, *Colloids and Surfaces A: Physicochemical and Engineering Aspects*, 394 (2012) 74-84.
- [26] M. Dabi, U.K. Saha, Application potential of vegetable oils as alternative to diesel fuels in compression ignition engines: A review, *Journal of the Energy Institute*, 92 (2019) 1710-1726.
- [27] E. Sharmin, F. Zafar, D. Akram, M. Alam, S. Ahmad, Recent advances in vegetable oils based environment friendly coatings: A review, *Industrial Crops and Products*, 76 (2015) 215-229.
- [28] M. Behzadnasab, S.M. Mirabedini, M. Esfandeh, R.R. Farnood, Evaluation of corrosion performance of a self-healing epoxy-based coating containing linseed oil-filled microcapsules via electrochemical impedance spectroscopy, *Progress in Organic Coatings*, 105 (2017) 212-224.
- [29] R.P. Wool, 4 - Polymers and composite resins from plant oils, in: R.P. Wool, X.S. Sun (Eds.) *Bio-Based Polymers and Composites*, Academic Press, Burlington, 2005, pp. 56-113.
- [30] H. Karatay, A. Sahin, O. Yilmaz, A. Aslan, Major Fatty Acids Composition of 32 Almond (*Prunus dulcis* (Mill.) D. A. Webb.) Genotypes Distributed in East and Southeast of Anatolia, *Turkish Journal of Biochemistry*, 39 (2014) 307-316.

- [31] M. Abdallah, I. Zaafarany, S. Wanees, R. Assi, Corrosion Behavior of Nickel Electrode in NaOH Solution and Its Inhibition by Some Natural Oils Authors: M. Abdallah, I. A. Zaafarany, S. Abd El Wanees and R. Assi Journal : Int.J.Electrochem Soc,9, 1071-1086(2014), International journal of electrochemical science, 9 (2014) 1071-1086.
- [32] Z. Ahmad, The uses and properties of almond oil, Complementary Therapies in Clinical Practice, 16 (2010) 10-12.
- [33] R. García-Cáceres, W. Aperador, A. Delgado-Tobón, Evaluation of the lubricating power of sweet almond oil without additives, DYNA, 85 (2018) 179 - 183.
- [34] M. Abdallah, I. Zaafarany, K.S. Khairou, Y. Emad, Natural oils as corrosion inhibitors for stainless steel in sodium hydroxide solutions, Chemistry and Technology of Fuels and Oils, 48 (2012) 234-245.
- [35] V. Kokol, M. Božič, R. Vogrinčič, A.P. Mathew, Characterisation and properties of homo- and heterogenously phosphorylated nanocellulose, Carbohydrate Polymers, 125 (2015) 301-313.
- [36] N. Inagaki, S. Nakamura, H. Asai, K. Katsuura, Phosphorylation of cellulose with phosphorous acid and thermal degradation of the product, Journal of Applied Polymer Science, 20 (1976) 2829-2836.
- [37] N. Illy, M. Fache, R. Ménard, C. Negrell, S. Caillol, G. David, Phosphorylation of bio-based compounds: the state of the art, Polymer Chemistry, 6 (2015) 6257-6291.
- [38] M. Ghanadpour, F. Carosio, P.T. Larsson, L. Wågberg, Phosphorylated Cellulose Nanofibrils: A Renewable Nanomaterial for the Preparation of Intrinsically Flame-Retardant Materials, Biomacromolecules, 16 (2015) 3399-3410.
- [39] G. Malucelli, Surface-Engineered Fire Protective Coatings for Fabrics through Sol-Gel and Layer-by-Layer Methods: An Overview, Coatings, 6 (2016) 33.
- [40] L.C. Corrêa-Filho, M. Moldão-Martins, V.D. Alves, Advances in the Application of Microcapsules as Carriers of Functional Compounds for Food Products, Applied Sciences, 9 (2019) 571.
- [41] V. Cortés, P. Talens, J.M. Barat, M.J. Lerma-García, Discrimination of intact almonds according to their bitterness and prediction of amygdalin concentration by Fourier transform infrared spectroscopy, Postharvest Biology and Technology, 148 (2019) 236-241.
- [42] S. Sharma, N. raj, FTIR Spectroscopic Characterisation of Almond Varieties (*Prunus dulcis*) from Himachal Pradesh (India), International Journal of Current Microbiology and Applied Sciences, 7 (2018) 887-898.
- [43] S. Hernández, F. Zacconi, Sweet almond oil: Extraction, characterization and application,

Química Nova, 32 (2008) 1342-1345.

- [44] F. Millet, R. Auvergne, S. Caillol, G. David, A. Manseri, N. Pébère, Improvement of corrosion protection of steel by incorporation of a new phosphonated fatty acid in a phosphorus-containing polymer coating obtained by UV curing, *Progress in Organic Coatings*, 77 (2014) 285-291.